PROCEEDINGS OF THE ROYAL SOCIETY A

Proc. R. Soc. A (2008) **464**, 2561–2573
doi:10.1098/rspa.2008.0009
Published online 20 May 2008

Enhancement of cloud formation by droplet charging

By R. Giles Harrison* and Maarten H. P. Ambaum

Department of Meteorology, University of Reading, PO Box 243, Earley Gate, Reading RG6 6BB, UK

Charge affects the activation of cloud droplets by reducing the minimum supersaturation at which haze droplets begin to grow. Although the droplet charge required to enhance activation is substantial, we show that sufficient charging occurs at the edges of layer clouds because the fair-weather current in the global atmospheric electrical circuit flows through a discontinuity in conductivity. Our theory predicts that droplet neutralization will cause a transient cooling of cloud base. This hypothesis was tested during a period of extreme solar activity, when we detected transient current bursts at the surface beneath a layer of cloud. We attribute these to bursts of ion production, which would cause transient droplet neutralization in the cloud and an associated increase in droplet critical supersaturation. We observed transient decreases in downward long-wave radiation measurements coincident with the transient current bursts. As the vertical current density passing through stratiform clouds is a global phenomenon, there are many regions in which a charge enhancement effect on cloud formation can potentially occur; we find that the effect of charge-enhanced activation on surface radiation in the present-day climate could be as large as 0.1 W m^{-2}.

Keywords: atmospheric electricity; solar variability and climate; cloud physics; electroactivation; cosmic rays

1. Introduction

Cosmic ray ion production is ubiquitous throughout the atmosphere and provides a major part of the ionization responsible for the electrical conductivity of atmospheric air (Bazilevskaya *et al.* in press). Away from the continental surface, galactic cosmic rays and their secondary particles dominate the production of molecular cluster ions in atmospheric air, which cause charging of aerosol particles and cloud droplets and facilitate vertical current flow between the ionosphere and the surface (Harrison & Carslaw 2003). Cluster ions consist of a central core ion, surrounded by polar molecules such as water. As galactic cosmic rays are modulated by solar activity, cosmogenic cluster ions may also link solar changes with weather and climate through clouds (Ney 1959; Dickinson 1975; Tinsley *et al.* 1989; Tinsley 2000; Carslaw *et al.* 2002; Harrison & Stephenson 2006). Cluster ions do not directly influence cloud droplet nucleation, however, because the water supersaturation is too small in atmospheric air (Mason 1971);

* Author for correspondence (r.g.harrison@reading.ac.uk).

Received 9 January 2008
Accepted 21 April 2008

but, in the middle and upper atmosphere, cluster ions can contribute to ultrafine particle nucleation (Lovejoy *et al.* 2004). The important role for cluster ions is in providing the finite electrical conductivity of atmospheric air, which permits vertical current flow between the ionosphere and the terrestrial surface within the global atmospheric electrical circuit (Rycroft *et al.* 2000). The air–earth conduction current (with current density $J_c \sim 1$ pA m^{-2}) is continuously present in non-thunderstorm regions and has been measured directly at the surface for over a century (Wilson 1906; Harrison & Ingram 2005).

The air–earth current density J_c responds to cloud, aerosol and global circuit changes on daily and seasonal time scales. Extreme solar events, however, such as solar flares, have been observed to cause substantial increases in J_c (Cobb 1967), on shorter time scales of hours. Energetic solar particle events (Bazilevskaya 2005) generate secondary particles in the atmosphere such as muons, electrons, protons, neutrons and photons. As secondary particles from galactic cosmic rays contribute to surface atmospheric ion production, secondary particles from high-energy solar or geomagnetic events are also expected to increase atmospheric ion production. There is evidence that solar events can enhance ion production rates in the lower atmosphere, and increased ion production from solar proton events has even been observed in mid-latitude surface ionization chambers. For example, the solar proton events of 23 February 1956 and 19 November 1949 caused large increases in neutron count rates in the UK (Shea & Smart 1995). These early cosmic ray measurements are of particular relevance owing to their use of ionization chambers, in which ion production is measured directly, rather than inferred to have occurred as would be the case with neutron counter measurements (Aplin *et al.* 2005). Shea & Smart (1995) also demonstrated ion production associated with a solar proton event in a surface ionization chamber, at Cheltenham, Maryland (39° N). This ionization was explained to be caused by muons, i.e. secondary particles generated from the solar protons. Other sources of high-energy particles in the lower atmosphere include thunderstorms (Wilson 1925; Lidvansky 2003), from which there is surface experimental evidence for accelerated electrons (Khaerdinov *et al.* 2005).

2. Electrical effects on clouds

To consider the influence of charged particles and their currents in the lower atmosphere further, we review some of the key physical cloud formation processes in which electrification could play a role. This discussion is restricted to the effects on layer (stratiform) clouds, under 'fair-weather' conditions, i.e. when no powerful local sources of charge separation, such as thunderstorms, are active.

(*a*) *Effects of droplet electrification on condensation*

Layer clouds arise through cooling of air parcels, usually following slow adiabatic ascent. The cooling increases the water supersaturation until, at the critical value, haze activates and grows into cloud drops, which we assume to occur principally at the cloud base. If the haze droplets are highly charged, their activation will occur at lower supersaturations, resulting in a lower cloud base temperature. The supersaturation S required for droplet formation, the critical supersaturation, can be found from Köhler theory (Mason 1971). For low droplet

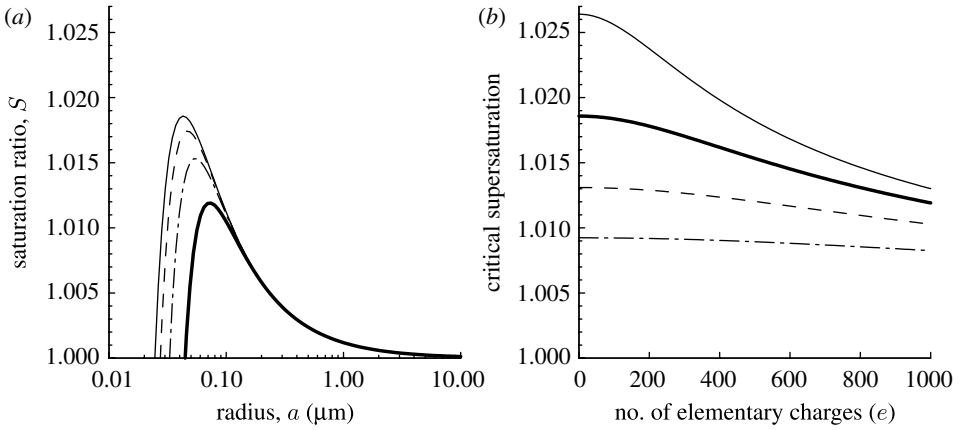

Figure 1. (*a*) Variation of saturation ratio S with droplet radius a, for j elementary charges carried by the droplet, with the critical supersaturation given by the turning point of each plotted line. (Quantities assumed: surface tension, 7.5×10^{-2} N m^{-1}; density, 1×10^{3} kg m^{-3}; dissolved salt amount, $M=5\times10^{-21}$ kg.) Thin solid line, $j=0$; dashed line, $j=250$; dot-dashed line, $j=500$; thick solid line, $j=1000$. (*b*) Sensitivity of the critical supersaturation to droplet charge, for different amounts M of dissolved salt (thin solid line, $M=2.5\times10^{-21}$ kg; thick solid line, $M=5\times10^{-21}$ kg; dashed line, $M=1\times10^{-20}$ kg; dot-dashed line, $M=2.5\times10^{-20}$ kg).

charges, the critical supersaturation is dominated by the dissolved salt contribution. At atmospheric supersaturations, which are typically less than 2% (i.e. $S\leq1.02$), it is well known that charge-enhanced activation of droplets requires very high droplet charges.

Figure 1*a* shows the calculations of the variation of saturation ratio S with particle radius, for a range of droplet charges, from Köhler theory, for droplets with a small dissolved salt contribution and a surface tension value assumed for pure water at 0°C (variation $\sim -0.2\%$ per °C, Mason 1971). It is clear from figure 1*a* that charging a haze droplet to 1000 elementary charges can reduce the critical supersaturation, by up to approximately 0.5%. Figure 1*b* shows the sensitivity of the critical supersaturation to droplet charge, for a range of dissolved salt contributions. The greatest sensitivity to charge is for droplets with a very small dissolved salt amount, such as pure water droplets forming on insoluble particles.

Consequently, we consider further the charging of haze and droplets on the edges of stratiform clouds.

(*b*) *Steady-state electrification on layer cloud boundaries*

Charging occurs at the boundary of layer clouds, as a result of the air–earth current density at the conductivity transition where the cloud forms (Tinsley 2000; Zhou & Tinsley 2007). (This is shown schematically in figure 2, illustrating the relevant properties that can be measured at the surface, the air–earth current density and the downwelling long-wave radiation.) To calculate the space charge density ρ at cloud base, we assume Ohm's Law ($J_c=\sigma E$, where E is the vertical electric field and σ the air conductivity) and Gauss' Law ($\mathrm{d}E/\mathrm{d}z=\rho/\varepsilon$, where ε is the permittivity). Such a one-dimensional approach is appropriate for stratiform

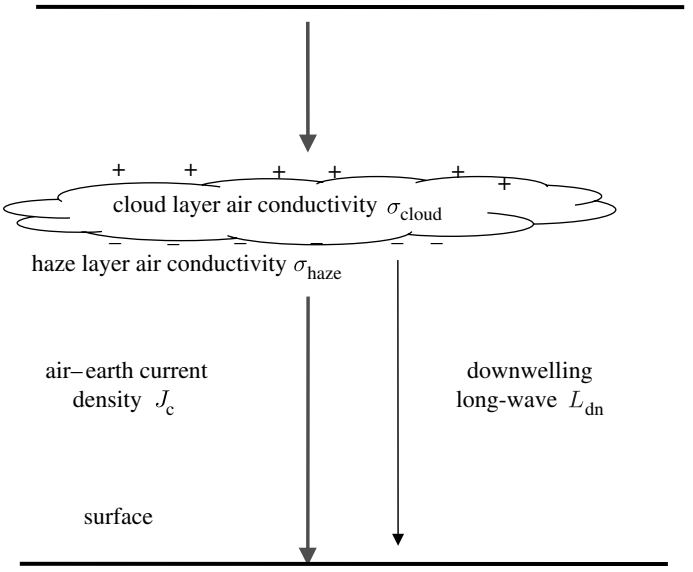

Figure 2. Effect of an extensive layer of cloud on the fair weather conduction current density J_c of the global atmospheric electric circuit. (The conduction current arises from the potential difference between the ionosphere and the surface, sustained by global thunderstorms and shower clouds.) The conduction current continues through the cloud layer, with charge accumulation on the cloud boundaries where the air conductivity σ changes sharply. Both the air–earth current density and the downwelling long-wave radiation from the cloud can be measured at the surface.

clouds of substantial horizontal extent above a horizontal surface. For quasi-steady background conditions, the vertical divergence of the current vanishes and ρ can be derived as

$$\rho = -\varepsilon J_c \frac{\mathrm{d}}{\mathrm{d}z}\left(\frac{1}{\sigma}\right), \tag{2.1}$$

with the total conductivity σ given by $\sigma = e(\mu_+ n_+ + \mu_- n_-)$ for $\mu_\pm$ the bipolar ion mobilities, $n_\pm$ the bipolar ion number concentrations and e the elementary charge. The bipolar ion concentrations $n_\pm$ are inversely proportional (Harrison & Carslaw 2003) to the radius-dependent ion-capture coefficients $\beta_\pm$ as $n_\pm = q/(Z\beta_\pm)$, for a given droplet concentration Z and volumetric ion production rate q. (Even within the cloud, the conductivity will be dominated by the residual ion concentrations, as the mobility of droplets is very much less than the ion mobilities.) Using established formulations (Gunn 1954) for β, it can be shown that

$$\sigma = \frac{2q\varepsilon}{|j|Z}\sinh(2\lambda|j|), \tag{2.2}$$

with j the number of elementary charges per droplet and $\lambda = e^2/(8\pi\varepsilon akT)$ for a the droplet radius, k Boltzmann's constant and T temperature.[1] As λj is small (Clement & Harrison 1992), $\sinh(2\lambda|j|)$ can be linearized, and it follows that

$$\frac{\sigma_{\text{haze}}}{\sigma_{\text{cloud}}} \geq \frac{a_{\text{cloud}}}{a_{\text{haze}}}, \tag{2.3}$$

[1] This result extends the first-order approximation in equation 18–38 of Pruppacher & Klett (1997).

for a_{cloud} and a_{haze} the cloud droplet and haze droplet radii, respectively, with the inequality arising from the contribution of the smaller haze particles to the conductivity. As haze and cloud droplet radii differ by more than an order of magnitude, the conductivity in cloud σ_{cloud} will be more than an order of magnitude less than that within the haze layer below. For $\sigma_{\mathrm{cloud}} \ll \sigma_{\mathrm{haze}}$, equation (2.1) can be approximated as $\rho \approx -(\varepsilon J_{\mathrm{c}})/(D\sigma_{\mathrm{cloud}})$ with D the depth of the haze to cloud transition layer. Assuming that all the cloud's charge is carried by the droplets, $\rho = -Zje$, which gives an implicit equation for j,

$$\sinh(2\lambda j) = \frac{J_{\mathrm{c}}}{2Deq}. \tag{2.4}$$

For $D \sim 1$–10 m, $a_{\mathrm{cloud}} \sim 10$–$100$ μm, $J_{\mathrm{c}} = (1$–$2)$ pA m^{-2} and $q = (2$–$5) \times 10^6$ ion pairs m^{-3} s^{-1}, we find j up to approximately 1000. (These values confirm our assumption that λj is small.) Such droplet charges would be sufficient to enhance the initial droplet activation, through the reduction of critical supersaturation noted earlier. Cloud droplets of $a = 3$ μm with $j = +1500$ have previously been observed at the base of mountain top stratocumulus clouds (Twomey 1956). Even in the presence of strong updraughts, which greatly diminish the peak charge, mean droplet charges of order $100e$ have been observed (Beard *et al.* 2004).

3. Observations

An opportunity to investigate the cloud changes associated with transient changes in atmospheric ionization was provided by measurements made during a solar storm on 14 December 2006, which culminated in an unusually energetic solar flare (ranked in the strongest category, X-class), late on 14 December. There were widespread reports of associated geomagnetic disturbances and aurorae (http://www.spaceweather.com), including from the southern UK at Hartland Observatory (51.0° N, 4.5° W), (http://www.geomag.bgs.ac.uk/bulletins/had/). During this solar event, a persistent anticyclone occurred over the UK. The low atmospheric variability resulting from the anticyclone provided an unusual opportunity for a direct investigation of transient ionization effects on lower atmosphere cloud. During the second half of 14 December, measurements of the air–earth current density J_{c} at Reading (51.4° N, 0.9° W) showed extremely high variability, considerably greater than that normally observed in steady meteorological conditions under the non-precipitating layer of cloud which was present.

Routine meteorological and atmospheric electrical observations were made at the Reading University Atmospheric Observatory (http://www.met.rdg.ac.uk/~fsdata/obshome.html) throughout the December 2006 solar event.

(*a*) *Instrumentation*

Air temperature and wind speed are measured automatically at Reading, alongside radiative quantities associated with the short-wave (solar) and long-wave (terrestrial) radiation flux densities. These variables include the short-wave direct and diffuse radiation and the upwards and downwards long-wave radiation. Wind speed and direction measurements are obtained from a Windmaster sonic anemometer, operated at 10 m. The principal radiation sensor

is a Kipp and Zonen CNR1 four-component radiometer. Signal voltages from the long-wave radiometers are retrieved using ultra low-noise amplifiers (Harrison & Knight 2006) with all sensors sampled at 1 Hz and 12 bit resolution, with the timing synchronized to the UK standard radio clock. The time response of the radiometers is typically 10–20 s, and 1 min averages are derived.

The atmospheric electricity observations include measurements of the potential gradient (PG), which is equal to $-E_z$, where E_z is the vertical component of the atmospheric electric field, and the vertical conduction current density (J_c). The PG measurement is obtained using a Chubb Instruments JCI131 field mill, standardized to the PG at 1 m above a horizontal surface. The currents received at two well-insulated horizontal collecting electrodes of different geometry are used to derive the conduction current density near the field mill. These two electrodes have cross-sectional areas of 0.140 and 0.276 m^2, the smaller of which is corrugated and the large one flat. Geometrical differences between the electrodes permit the conduction current density to be found, with the error term from displacement currents arising from electric field changes removed (Bennett & Harrison 2006, 2008). Both the collecting electrodes have a 33 s low-pass filter, and 1 min averages have been derived from the 1 s samples.

(*b*) *Data summary*

Figure 3 summarizes measurements on 14 and 15 December at Reading during which a stratiform liquid water cloud was permanently present. At Chilbolton (50 km from Reading), the cloud base was measured to be 800 m using light detection and ranging (lidar). Figure 3*a* shows the horizontal (u) and vertical (w) wind speeds and temperature (T) measured over the 2 days and figure 3*b* shows the downwelling long-wave radiation (L_{dn}). The temperature trace illustrates the small amplitude diurnal cycle in December, varying by less than 2°C, and the L_{dn} also exhibits little variability. The air–earth current density J_c, derived from the measured currents (Harrison 1997) flowing to each of the two well-insulated electrodes, is shown in figure 3*c*, together with the PG. Importantly, the substantial variations in J_c occur when L_{dn} is steady, which allow the effects of J_c on the cloud to be studied.

Both electrode currents exhibited increased variability from the middle of 14 December and, unusually, substantial instantaneous currents of both polarities thereafter. Some context is given by 722 hours of fair weather data in September and October 2006, during which the median J_c was 1.8 pA m^{-2} (range 0.2–4 pA m^{-2}). On the morning of 14 December, the median J_c was 1.3 pA m^{-2}, but on the afternoon of 14 December, the variability greatly increased to span -10.8 to 12.1 pA m^{-2}. Figure 4*a* shows histograms of the 1 min mean J_c measurements obtained on the morning and afternoon of 14 December. It is apparent that the J_c measurements on the afternoon and evening of 14 December have a much broader distribution than during the morning. The afternoon and evening of 14 December had an appreciable number of negative J_c values, as well as more J_c values between 2 and 5 pA m^{-2}, compared with the morning before. To remove the effects of slow changes occurring in cloud or the global circuit, all the 1 min values on days 348 and 349 have been filtered with a 60 min Lanczos high-pass filter. Figure 4*b* shows a histogram of values obtained after the high-pass filtering, which clearly illustrates the wide range of values that occurred.

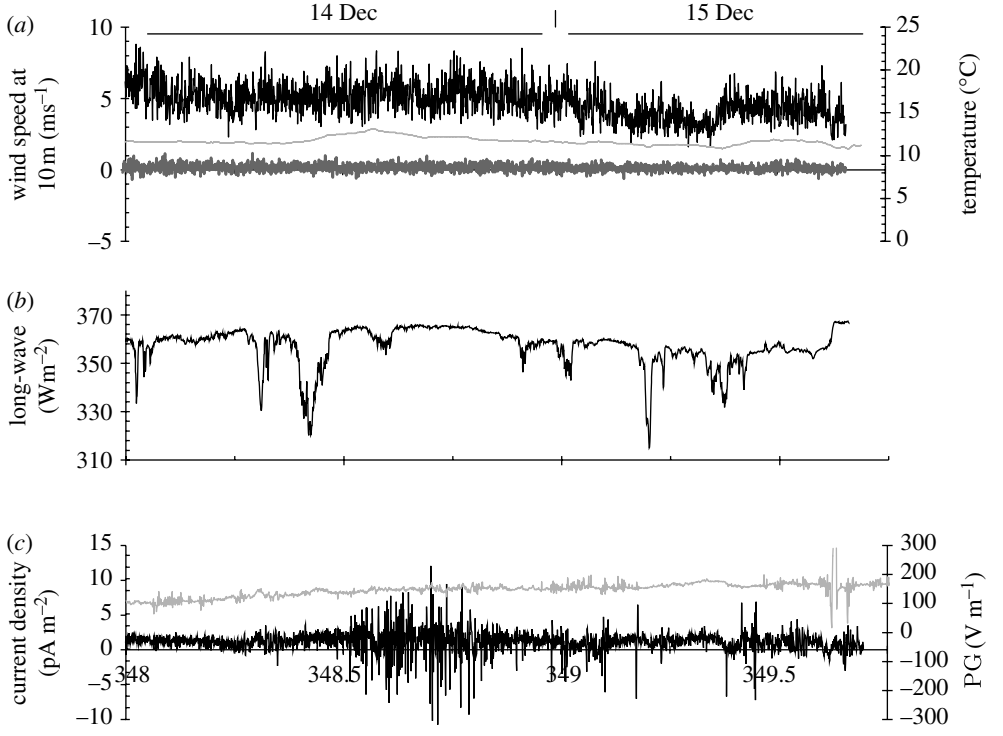

Figure 3. Surface measurements made at Reading during 14 and 15 December 2006 (days of year 348 and 349, respectively) of: (*a*) horizontal wind speed (black) and vertical wind speed (thick dark grey line) at 10 m, and surface air temperature (thin dark grey line), (*b*) downwards long-wave radiation, and (*c*) the air–earth current density (black) and potential gradient (PG; grey) at 1 m. (All quantities are 1 min averages.)

(*c*) *Origin of variability in the conduction current density*

The unusual variability in conduction current provides strong evidence for exceptional atmospheric electrical conditions on 14 December 2006. The negligible meteorological variability evident from u, w and T and the absence of any observed precipitation make it difficult to attribute the J_c variability to meteorological changes.

Alternatives are that the J_c variability arose from (i) an instrument failure or (ii) sub-visible charged water droplets arriving at the electrodes. Possibility (i), instrument failure, is highly unlikely owing to the close agreement in currents measured at the two independent electrodes, and therefore a coincident failure would be required. (Both electrode insulators had been cleaned on the afternoon of 13 December.) Possibility (ii), sub-visible precipitation, can be rejected for several reasons. Firstly, even during light liquid rainfall, substantial fluctuations (Bennett & Harrison 2007) occur in the PG, and, commonly, a reversal (Chalmers 1967) in the PG's sign occurs: neither was recorded (figure 3*c*). Secondly, ohmic conduction links positive (fair weather) PG values with positive J_c values. As the $J_c<0$ values generally occurred without a reversal of sign in the PG, this suggests that no charged droplets were present to be detected by the field mill, despite it being adjacent to the J_c apparatus. Thirdly, the relative humidity near the surface

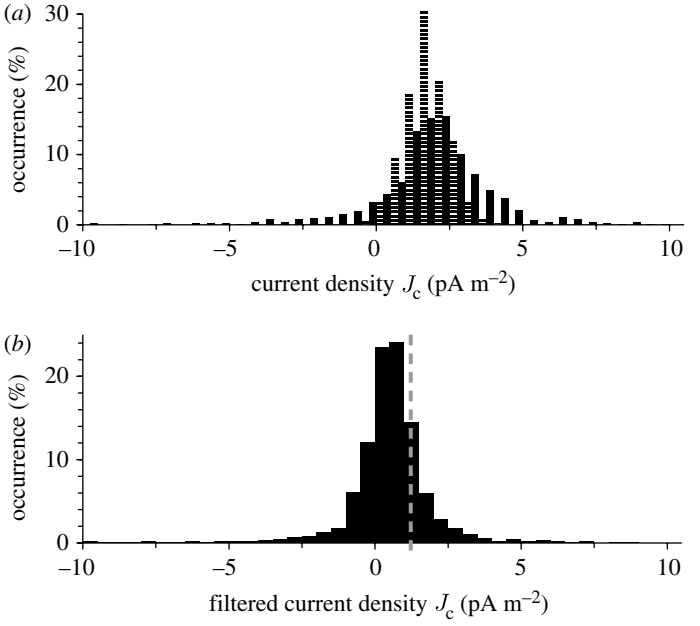

Figure 4. Histograms of 1 min air–earth current density measurements for (*a*) each half of day 348 (14 December 2006; horizontally lined bars, morning; black filled bars, afternoon) and (*b*) all 1 min air–earth current density values on days 348 and 349, after high-pass filtering (dashed line marks the upper decile, which begins at $J_c = 1.28$ pA m^{-2}).

was well below saturation (between 75 and 83% with median 80%) throughout the second half of 14 December, indicating that any droplets would evaporate before reaching the surface.

Careful examination of individual fluctuations in the raw (1 s) current data (not shown) from the collecting electrodes showed, in many cases, that both electrodes were affected by the increased variability. For some of the slower fluctuations, common changes were also apparent in the PG data, but some of the more rapid changes were not detected by the field mill, even though it had a considerably faster time response than the current-collecting electrodes with their long time constant. (The field mill response is specified by the manufacturer to have halved from its DC value to oscillatory signals at approx. 7 Hz.) Charge transfer was therefore occurring rapidly in those circumstances. Owing to the absence of precipitation conveying charge to the electrodes, and no conduction process evident from the field mill or current collecting electrodes in some of the fluctuations, we conclude that some of the charge pulses arose from charged particles reaching the bottom of the atmosphere ballistically.

4. Analysis of observations

An experimental test of the charge effect on haze activation was provided by the air–earth current variability on 14 December, as co-located surface measurements of long-wave radiation—providing simultaneous cloud information—are available. Evidence for a change in cloud base temperature can be inferred from

surface measurements of the long-wave radiation flux density emitted from the cloud. Cloud base temperature could also be interpreted as a measure of the cloud base altitude, given a fixed vertical temperature profile. However infrared absorption by water vapour below the cloud is expected to mask some of the cloud variations in L_{dn} measured at the surface. Consequently, any inferred variations in L_{dn} represent a lower limit of the cloud base changes.

(*a*) *Possible cloud droplet changes*

Suddenly enhanced production of ions in the cloud region during peaks in J_{c} would temporarily have sharply increased the local air conductivity, as this is proportional to the ion concentration for constant ion mobility. These increases would only ever be temporary, as the ions will be captured by the droplets over a time scale of several minutes. Owing to the conductivity increase, the haze droplet charge would be transiently reduced, removing the electrical enhancement of droplet activation. (Equation (2.4) shows that, for the steady-state case, increasing q reduces j.) As a result, we would expect haze activation to have occurred at greater critical supersaturation, causing the cloud base radiating temperature to decrease.

The time scales for discharging and charging of the haze determine, respectively, the time scale for the reduction of activation and return to the electrically enhanced activation level. The discharging (or charging) time scale is $1/\beta Z$. β is greater for highly charged haze than for discharged haze, hence the time scales are asymmetric: the discharging time scale for highly charged haze is very rapid (approx. 1–10 s) but the charging time scale for near-neutral haze is typically approximately 100 s.

From Stefan–Boltzmann's equation, the fractional change in long-wave radiation flux density is expected to be several times greater than the fractional change in cloud temperature, and exactly four times greater if the atmosphere has no absorbing effect. The change in measured surface long-wave radiation flux density therefore provides a sensitive measure of the change in cloud base temperature. Fortuitously, the longer time-scale component of the L_{dn} variability was small during the days concerned, owing to steady cloud conditions. Figure 5*a*,*b* shows time series of the 1 min average L_{dn} and J_{c}, after the high-pass filtering, which are used for subsequent analysis of rapid cloud changes. Figure 5*c* also shows measurements made of the earthward magnetic field by the GOES-12 satellite; the magnetic storm occurs at a similar time to the strong variability in the air–earth current measurements. This is further evidence that the measured current event had a geophysical origin, rather than a local meteorological fluctuation or apparatus malfunction.

(*b*) *Compositing of extreme events*

To investigate cloud changes, we consider that the extreme J_{c} values present during the measurements result from high-energy particle precipitation events and therefore study their coherency with L_{dn} variations. As the currents generated at the air–earth current electrodes were sufficiently small as to require a sensitive electrometer for their measurement, it is not conceivable that such small currents could influence the radiometer or their amplifiers directly, as they operate with currents many orders of magnitude greater.

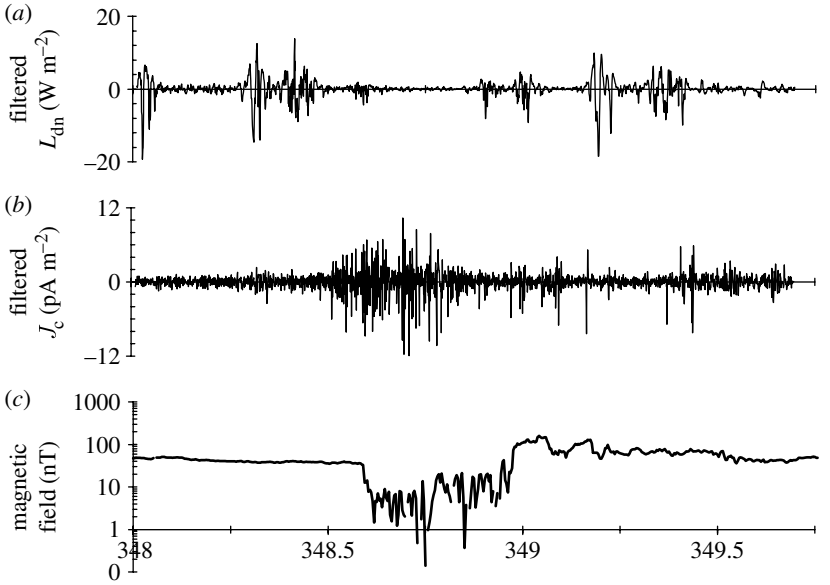

Figure 5. High-frequency fluctuations in (*a*) L_{dn} and (*b*) J_c, respectively, after high-pass filtering the raw time series (day 348=14 December 2006). (*c*) The earthward magnetic field, as measured by the GOES-12 satellite (75° W).

Furthermore, four identical radiometer amplifiers were in use at the site, including one for the measurement of L_{up} using the same radiometer instrument containing the L_{dn} sensor. The non-L_{dn} amplifiers showed no response coherent with the J_c variations.

The method used to study the cloud's radiative response to large J_c changes is to extract fixed length sections of the L_{dn} time series centred around every J_c fluctuation above a chosen size, which are then averaged. The average found represents the mean radiative response to J_c fluctuations. This approach ('compositing') allows the typical lag time between an initiating event and its response to be found, compared with the variability present. Based on the histogram in figure 4, we selected the upper decile of filtered J_c values to provide the extreme values on which to composite multiple events. This provided 226 upper decile measurements, with high-pass filtered $J_c > 1.28$ pA m^{-2} (figure 4*b*). The simultaneous L_{dn} measurements were also composited using the same J_c (upper decile) values. Figure 6*a* shows the composite time series for the filtered J_c data. We find that, at the event time ($t=0$), the mean (filtered) J_c is (2.47 ± 0.1) pA m^{-2}. The decorrelation of J_c is rapid, of the order of 1 sample (1 min), but the negative flanks before and after the event imply spectral power at or above the 1 min time scale.

Figure 6*b* shows the rate of change in L_{dn} (from centred differences), coincident with the J_c events. The L_{dn} rate of change composite immediately shows a $-(0.31 \pm 0.08)$ W m^{-2} min^{-1} (3.9 s.e.) response, followed by a slower recovery lasting several minutes. As explained in §4*a*, the charging and discharging time scales are expected to be asymmetric, with the initial discharging rapid (less than 1 min) and the subsequent recharging slower (several minutes).

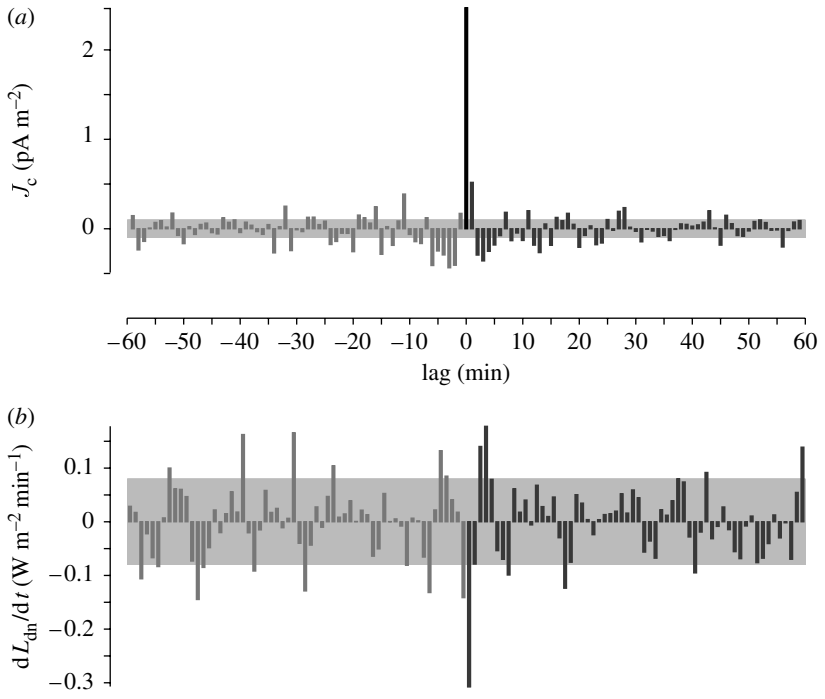

Figure 6. (*a*) A composite of the high-pass (leaving periods shorter than 60 min) filtered current density J_c, composited on the upper decile of these values (representing the high-energy transient events). (*b*) The equivalent composite for the mean rate of change (centred difference) of the high-pass filtered downward long-wave radiation flux density L_{dn}. (For either time series, the grey background shading represents ± 1 s.e.)

Standard errors are used as the composite is an average of a selection of the measurements which, outside the decorrelation time,[2] can be considered independent. The central limit theorem then states that, outside the decorrelation time, the composites have a Gaussian distribution. Additionally, from inspection of the composite values in the long time window in figure 6, it is clear that the signals around zero lag are highly significant.

5. Discussion

The change observed (a reduction of 0.3 W m^{-2} in the downward long-wave radiation) illustrates a small but systematic effect of droplet electrification on cloud base temperature, through the reduction in critical supersaturation facilitated by the charging of droplets. A transient removal of the droplet charge causes the critical supersaturation to be increased. The amount of droplet charging therefore modulates the conditions which define where the cloud base forms.

[2] We also assume that each selection represents a sufficiently small sample of the whole time series for the samples to be considered independent.

The radiative change can also be considered in terms of the change in cloud base temperature. For a 0.3 W m^{-2} reduction in 350 W m^{-2}, the corresponding fractional reduction in absolute temperature would be approximately 1 in 5000, or approximately 0.06 K at cloud temperature. In moist air, a 0.06 K decrease would typically correspond to a cloud base altitude increase of approximately 10 m. This estimate was investigated in separate measurements made at Chilbolton using direct cloud height (ceilometer) measurements: for Chilbolton on 15 December 2006, the linear relationship between L_{dn} and cloud height showed a 24 m increase in cloud base for a 0.3 W m^{-2} reduction. The approximately 10 m change is therefore likely to be conservative, but it will depend closely on the specific cloud properties in other circumstances.

Because vertical air–earth conduction current is present globally, the abundance of stratiform clouds implies extensive regions globally where cloud edge droplet charges may influence haze activation and modulate the cloud base. Such regions would experience cloud edge modulation from global atmospheric electrical circuit changes and cosmic rays. Daytime observations show that stratus, altostratus and stratocumulus clouds cover approximately 22% of the planet's area (http://isccp.giss.nasa.gov/climanal.html). Consequently, if the (0.31 ± 0.08) W m^{-2} reduction observed represents complete droplet neutralization, and geomagnetic changes can be neglected, the global circuit's charging effect on activation in stratiform cloud would amount to a positive contribution to the global radiation budget of (0.07 ± 0.03) W m^{-2}, where the uncertainty represents two standard errors.

Dr A. J. Bennett provided the air–earth current and PG measurements and A. G. Lomas maintained the radiation instruments.

References

Aplin, K. L., Harrison, R. G. & Bennett, A. J. 2005 Effect of the troposphere on surface neutron counter measurements. *Adv. Space Res.* **35**, 1484–1491. (doi:10.1016/j.asr.2005.02.055)

Bazilevskaya, G. A. 2005 Solar cosmic rays in the near Earth space and the atmosphere. *Adv. Space Res.* **35**, 458–464. (doi:10.1016/j.asr.2004.11.019)

Bazilevskaya G. A. *et al.* In press. Cosmic ray induced ion production in the atmosphere. *Space Sci. Rev.* (doi:10.1007/s11214-008-9339-y)

Beard, K. V., Ochs, H. T. & Twohy, C. H. 2004 Aircraft measurements of high average charges on cloud drops in layer clouds. *Geophys. Res. Lett.* **31**, L14 111. (doi:10.1029/2004GL020465)

Bennett, A. J. & Harrison, R. G. 2006 Surface determination of the air–earth electrical current density using co-located sensors of different geometry. *Rev. Sci. Instrum.* **77**, 066 104. (doi:10.1063/1.2213210)

Bennett, A. J. & Harrison, R. G. 2007 Atmospheric electricity in different weather conditions. *Weather* **62**, 277–283.

Bennett, A. J. & Harrison, R. G. 2008 Surface measurement system for the atmospheric electrical vertical conduction current density, with displacement current correction. *J. Atmos. Solar-Terr. Physics* **70**, 1373–1381. (doi:10.1016/j.jastp.2008.04.014)

Carslaw, K. S., Harrison, R. G. & Kirkby, J. 2002 Cosmic rays, clouds and climate. *Science* **298**, 1732–1737. (doi:10.1126/science.1076964)

Chalmers, J. A. 1967 *Atmospheric electricity*, 2nd edn. Oxford, UK: Pergamon.

Clement, C. F. & Harrison, R. G. 1992 The charging of radioactive aerosols. *J. Aerosol. Sci.* **23**, 481–504. (doi:10.1016/0021-8502(92)90019-R)

Cobb, W. E. 1967 Evidence of a solar influence on the atmospheric electric elements at Mauna Loa Observatory. *Mon. Weather Rev.* **95**, 905–911. (doi:10.1175/1520-0493(1967)095<0905:EOASIO>2.3.CO;2)

Dickinson, R. E. 1975 Solar variability and the lower atmosphere. *Bull. Am. Meteorol. Soc.* **56**, 1240. (doi:10.1175/1520-0477(1975)056<1240:SVATLA>2.0.CO;2)

Gunn, R. 1954 Diffusion charging of atmospheric droplets by ions and the resulting combination coefficients. *J. Meteorol.* **11**, 339–347.

Harrison, R. G. 1997 A noise-rejecting current amplifier for surface atmospheric ion flux measurements. *Rev. Sci. Instrum.* **68**, 3563–3565. (doi:10.1063/1.1148323)

Harrison, R. G. & Carslaw, K. S. 2003 Ion–aerosol–cloud processes in the lower atmosphere. *Rev. Geophys.* **41**, 1012. (doi:10.1029/2002RG000114)

Harrison, R. G. & Ingram, W. J. 2005 Air–earth current measurements at Kew, London, 1909–1979. *Atmos. Res.* **76**, 49–64. (doi:10.1016/j.atmosres.2004.11.022)

Harrison, R. G. & Knight, J. R. 2006 Thermopile radiometer signal conditioning for surface atmospheric radiation measurements. *Rev. Sci. Instrum.* **77**, 116 105. (doi:10.1063/1.2370752)

Harrison, R. G. & Stephenson, D. B. 2006 Empirical evidence for a nonlinear effect of galactic cosmic rays on clouds. *Proc. R. Soc. A* **462**, 1221–1233. (doi:10.1098/rspa.2005.1628)

Khaerdinov, N. S., Lidvansky, A. S. & Petkov, V. B. 2005 Cosmic rays and the electric field of thunderclouds: evidence for acceleration of particles (runaway electrons). *Atmos. Res.* **76**, 346–354. (doi:10.1016/j.atmosres.2004.11.012)

Lidvansky, A. S. 2003 The effect of the electric field of the atmosphere on cosmic rays. *J. Phys. G: Nucl. Part. Phys.* **29**, 925–937. (doi:10.1088/0954-3899/29/5/313)

Lovejoy, E. R., Curtius, J. & Froyd, K. D. 2004 Atmospheric ion-induced nucleation of sulfuric acid and water. *J. Geophys. Res.* **109**, D08204. (doi:10.1029/2003JD004460)

Mason, B. J. 1971 *Physics of clouds*. Oxford, UK: Pergamon.

Ney, E. P. 1959 Cosmic radiation and the weather. *Nature* **183**, 451–452. (doi:10.1038/183451a0)

Pruppacher, H. R. & Klett, J. D. 1997 *Microphysics of clouds and precipitation*, 2nd edn. Dordrecht, The Netherlands: Kluwer Academic Publishers.

Rycroft, M. J., Israelsson, S. & Price, C. 2000 The global atmospheric electric circuit, solar activity and climate change. *J. Atmos. Sol. Terr. Phys.* **62**, 1563–1576. (doi:10.1016/S1364-6826(00)00112-7)

Shea, M. A. & Smart, D. F. 1995 History of solar proton even observations. *Nucl. Phys. B* (*Proc. Suppl.*) **39A**, 16–25. (doi:10.1016/0920-5632(95)00003-R)

Tinsley, B. A. 2000 Influence of solar wind on the global electric circuit, and inferred effects on cloud microphysics, temperature, and dynamics in the troposphere. *Space Sci. Rev.* **94**, 231–258. (doi:10.1023/A:1026775408875)

Tinsley, B. A., Brown, G. M. & Scherrer, P. H. 1989 Solar variability influences on weather and climate: possible connections through cosmic ray-fluxes and storm intensification. *J. Geophys. Res.* **94**, 14 783–14 792. (doi:10.1029/JD094iD12p14783)

Twomey, S. 1956 The electrification of individual cloud droplets. *Tellus* **8**, 445–451.

Wilson, C. T. R. 1906 On the measurement of the earth–air current and on the origin of atmospheric electricity. *Proc. Camb. Philos. Soc.* **13**, 363–382.

Wilson, C. T. R. 1925 The acceleration of β-particles in strong electric fields such as those of thunderclouds. *Proc. Camb. Philos. Soc.* **22**, 534–538.

Zhou, L. & Tinsley, B. A. 2007 Production of space charge at the boundaries of layer clouds. *J. Geophys. Res.* **112**, D11203. (doi:10.1029/2006JD007998)